Electric Field Assisted-Assembly of Perpendicular Oriented ZnO Nanorods on Si Substrate

O. Lupan[*,**], L. Chow[**], G. Chai[***], S. Park[**] and A. Schulte[**]

[*]Technical University of Moldova, Blvd. Stefan cel Mare 168, Chisinau MD-2004, Moldova, lupanoleg@yahoo.com
[**]Department of Physics, University of Central Florida, Orlando, PO Box 162385, FL, USA, chow@mail.ucf.edu lupan@physics.ucf.edu
***Apollo Technologies, Inc., 205 Waymont Court, 111, Lake Mary, FL 32746, USA, guangyuchai@yahoo.com

ABSTRACT

In this work, we report a new electric-field assisted assembly technique used to vertically-align ZnO nanorods on the Si substrate during their growth. In the assembly process, the forces that induce the alignment are a result of the polarization of the electric field. The synthesis was carried out at near-room temperature (90° C). Novel measurements on these structures show encouraging characteristics for future applications.

The phase purity, composition and morphology of the synthesized products by the assembly method were examined by XRD, TEM, and SEM. Room-temperature micro-Raman spectroscopy was performed to examine the properties of the self-assembly ZnO nanorods on Si substrate structures. Such highly oriented and ordered ZnO nanorods could be beneficial for field emission, solar cells, LEDs and spintronic applications.

Keywords: ZnO nanorod, self-assembly, nanorod arrays, nanowires, silicon

1 INTRODUCTION

ZnO is of importance for fundamental research as well as relevant to industrial and high-technology applications. ZnO can also be considered as an alternative wide band gap semiconductor for photonic devices [1]. ZnO nanorods/nanowires are becoming common building blocks for the next generation electronic devices [2].

In this context, self - assembly and assisted - assembly of nano-architectures has attracted high interest driven by the demands of technology and engineering. The large interest is motivated by necessity in development of new fabrication tools for novel electronic, optoelectronic and magnetic properties for versatile applications in nanotechnology. Chemical and electric field assisted-assembly offer a new opportunity to create heterostructures in multicomponent systems and to manufacture of nanodevices. They include nanorods-based ultra-violet lasers [3], nanosensors [2] and light emitting diodes [4, 5] with higher performances and significantly lower cost in comparison to the traditional lithographic fabrication. Thus, it is important to study the novel fabrication techniques of semiconducting nanorods-nanowires for future applications.

At the same time, from a fundamental point of view, it is crucial to study the structure and assembly of such novel materials to enable tailoring their properties for novel and improved nanodevices fabrication. Efficient manipulation, positioning and alignment of one-dimensional (1-D) ZnO nanowires present key challenges toward the integration of nanostructures with larger scale systems.

The presence of a direct current (DC) electric field during synthesis yields a better organized growth, because nanorods will align with electric-field lines. This behavior can be attributed to the polarizability of 1-D nanorods and the electrophoretic effect [6].

ZnO nanoarchitectures can be assembled on different types of substrates (e.g. glass, silicon, sapphire) by patterning the seed or catalyst layer, and usually the ZnO nanorods are well-aligned with their *c*-axis perpendicular to the substrate surface [3]. In this respect, typically gold is used to catalyze the growth of nanorods from vapor–liquid–solid (VLS) method and silver is used to facilitate the assembly of ZnO nanorods from solution [7, 8].

In this paper, we demonstrate electric field assisted-assembly of perpendicularly oriented ZnO nanorods on a Si substrate during growth from aqueous solution. We demonstrate the flexibility to order ZnO nanorods on substrates through the strength of the electric field.

2 EXPERIMENTAL

The starting materials, zinc sulfate ($Zn(SO_4)\cdot 7H_2O$, 99.9 % purity) and ammonia NH_4OH (29.6%) were used as received without further purification.

The hydrothermal synthesis of vertically-aligned ZnO nanorod arrays was carried out by dissolving $Zn(SO_4)\cdot 7H_2O$ and ammonia NH_4OH (29.6%) in 20 mL of deionized water (18.2 MΩ·cm). The complex solution was then transferred to a reactor [9]. A DC electric field was applied during growth. The substrates, Si or glass slides were placed in

vertical and horizontal positions in order to study the effect of the electric field direction on the synthesized samples. The reactor was heated at 90 °C for 20 min and then cooled to 40 °C.

After synthesis, substrates were washed with distilled water several times and then dried in a hot air flux at 150 °C. ZnO nanorods with different architectures were also prepared with the same procedure.

X-ray diffraction (XRD) pattern were obtained with a Rigaku 'D/B max' diffractometter, CuK_α radiation (λ=1.54178 Å) were used, operating at 40 kV and 30 mA. All samples were measured in a continuous scan mode at 20 – 90 ° (2θ) with a scanning range of 0.01°/s). Peak positions and relative intensities of synthesized nanorod arrays were compared to values from Joint Committee on Powder Diffraction Standards (JCPDS) card for ZnO (JCPDS 036-1451) [10].

The morphology of the products was obtained using a scanning electron microscope (SEM, JEOL and a Hitachi S800) and high resolution transmission electron microscopy (TEM) (FEI Tecnai F30 TEM). Room-temperature micro-Raman spectroscopy experiments were performed with a Horiba Jobin Yvon LabRam IR system at a spatial resolution of 2 μm. Raman scattering was excited with the 633 nm line of a He-Ne laser with less than 4 mW of power at the sample.

3 RESULTS AND DISCUSSION

The phase composition and phase purity of ZnO nanorods were identified by XRD analysis. Typical patterns are depicted in Fig. 1. All diffraction peaks of the products are well indexed as the hexagonal phase of wurtzite zinc oxide (space group $P6_3mc$(186); a = 0.32498 nm, c = 0.52066 nm, JCPDS card #036-1451). The cell parameters of a and c of obtained samples are 3.2502 Å and 5.2096 Å calculated by using the following equation [9]

$$\frac{1}{d^2_{(hkl)}} = \frac{4}{3}\left(\frac{h^2+hk+k^2}{a^2}\right)+\frac{l^2}{c^2} \qquad (1)$$

using the d_{hkl} measured on the XRD pattern. From Fig. 1(a) for ZnO nanorods on Si grown under electric field assistance, only diffractive peaks in the pattern which belong to ZnO wurtzite structure were observed. The full width of half maximum (FWHM) of (002) diffraction peak is only 0.51°. Thus, Fig. 1(a) shows the X-ray diffraction patterns determined by the (002) plane, indicating that zinc oxide has a single ZnO phase.

Fig. 1(b) shows the X-ray diffraction pattern for ZnO nanorods on Si grown without electric field assistance. It can be observed that the sample has a good crystalline phase, but dominated by the (101) plane. From the Fig. 1 one can conclude that all intensities indicate the good crystalline ZnO material.

The typical morphology of the ZnO nanorods on glass prepared by hydrothermal synthesis after the growth time of 20 min is shown in Fig. 2(a). All products are hexagonal nanorods with closed ends (see inset Fig 2(a)). The radius of nanorods is around 400 nm and the length is about 2-3 μm. These ZnO nanorods are randomly distributed on the substrate.

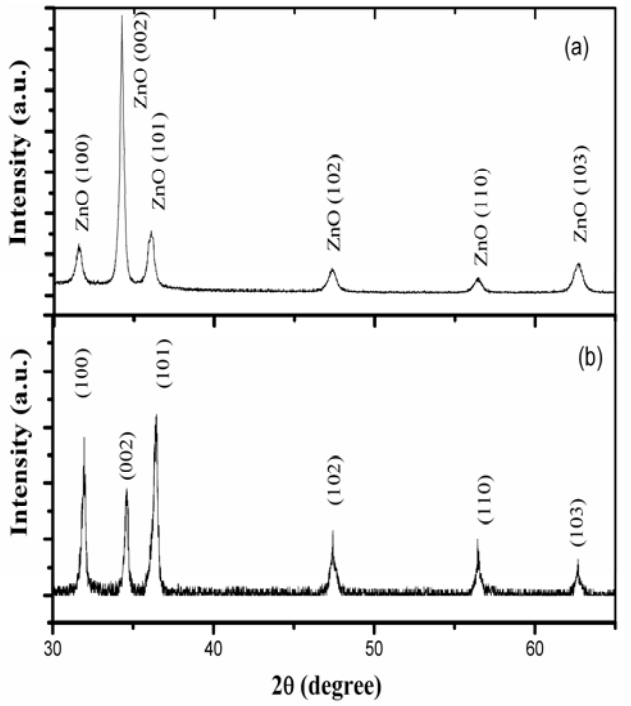

Figure 1: XRD patterns of (a) quasi-aligned ZnO nanorods on Si grown under electric field assistance and (b) ZnO nanorods on Si grown without electric field assistance.

An enlarged SEM view in the inset of Fig. 2(b) illustrates hexagonal symmetry of ZnO nanorods on Si grown under relatively weak electric field (~$5\cdot10^3$ V/m) assistance. The alignment of ZnO nanorods on Si(111) substrate as shown in Fig. 2(c) increases under stronger electric field (~$5\cdot10^4$ V/m) assistance. The diameter and length of the nanorods (Fig 2c) are smaller than those grown on glass substrates (Fig 2a). The radius is about 100 nm and can be observed that all have the same dimensions.

The perpendicular orientation of the ZnO nanorods is controlled by the electric field, but lattice match between the two materials may play a role. The lattice mismatch between ZnO and Si (111) is ~3.5% [11]. Based on the observed nanorod growth from SEM image (Fig 2c), it is concluded that stronger fields will contribute to better alignment. At the same time we notice that some ZnO nanorods grow at a slightly inclined angle. Comparing with glass substrates the mosaic distribution is narrower for Si. But slightly tilted ZnO nanorods can be observed on the Si substrate.

NSTI-Nanotech 2008, www.nsti.org, ISBN 978-1-4200-8503-7 Vol. 1

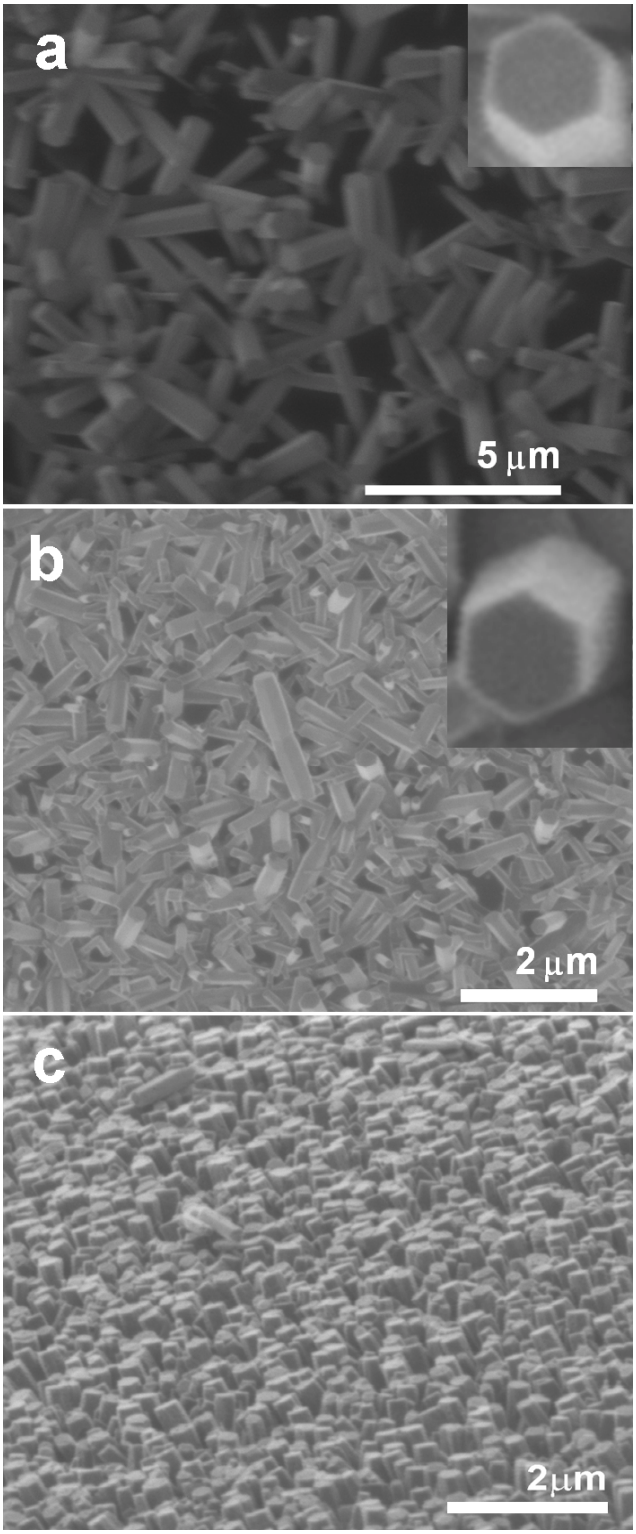

Figure 2: SEM images of (a) ZnO nanorods on glass substrate, (b) ZnO nanorods on Si substrate grown under relatively weak electric field assistance and (c) quasi-aligned ZnO nanorods on Si wafers grown under stronger electric field assisted-assembly.

Therefore, the ZnO nanorods reflect more uniformity and vertical alignment on Si compared to glass substrate. In order to study the vibrational properties of the ZnO nanorod arrays room-temperature Raman measurements were performed. The spectral shape and the peak position of the Raman shift are related to the crystallinity, structural disorder, residual stress, and defects in the investigated samples. Figure 3 shows the micro-Raman spectrum of ZnO nanorods on Si substrates with growth time of 20 min on glass without assistance and on the Si under stronger electric field assisted-assembly. The wurtzite phase ZnO belongs to C_{6v}^4 or 6*mm* symmetry group. All observed peaks can be assigned to phonon modes which correspond to those of ZnO [13].

The optical phonons at the Γ point in the Brillouin zone belong to the representation [14]:

$$\Gamma_{opt} = 1A_1 + 2B_1 + 1E_1 + 2E_2 . \quad (1)$$

A_1 and B_1 modes are polar and split into transverse optical (TO) and longitudinal optical (LO) phonons with different frequencies due to the macroscopic electric fields associated with the LO phonons. The interatomic forces can cause anisotropy, that's why A_1 and E_1 modes have different frequencies. Due to the fact that the electrostatic forces dominate the anisotropy in the short–range forces, the TO–LO splitting is larger than the A_1 E_1 splitting. In the case of lattice vibrations with A_1 and E_1 symmetry, the atoms move perpendicular and parallel to the *c*–axis, respectively. The A_1 and E_1 modes are Raman and infrared (IR) active. The non-polar IR inactive E_2 (E_2(low), E_2(high)) modes are Raman active. The B_1 modes are IR and Raman inactive (silent modes). From group theory the $A_1 + E_1 + 2E_2$ modes are Raman active.

The peak at 438 cm^{-1} (Fig. 3 a and b) is attributed to E_2(high) mode of non-polar optical phonons, which is a characteristic Raman active branch of hexagonal ZnO. The strong E_2(high) mode demonstrates that the ZnO nanorods are of good crystalline hexagonal structure which corroborates with XRD data (Fig 1a).

Compared to bulk material the E_2(high) mode show a 1cm^{-1} blue-shift. One of the reasons is that nanorods possess piezoelectric effect which causes the shift of Raman modes. Another one can be attributed to the optical-phonon confinement (which is anisotropic and has different effect on different phonon modes). Also shift can be attributed to the strain variation.

As E_2(high) mode is close to that of bulk ZnO (437-439 cm^{-1}), the sample with oriented nanorod arrays can be regarded as unstrained. The peak at 332 cm^{-1} corresponds the E_{2H}-E_{2L} mode and shows broadening (about 70 cm^{-1}) (Fig. 3b) due to multiphonon processes.

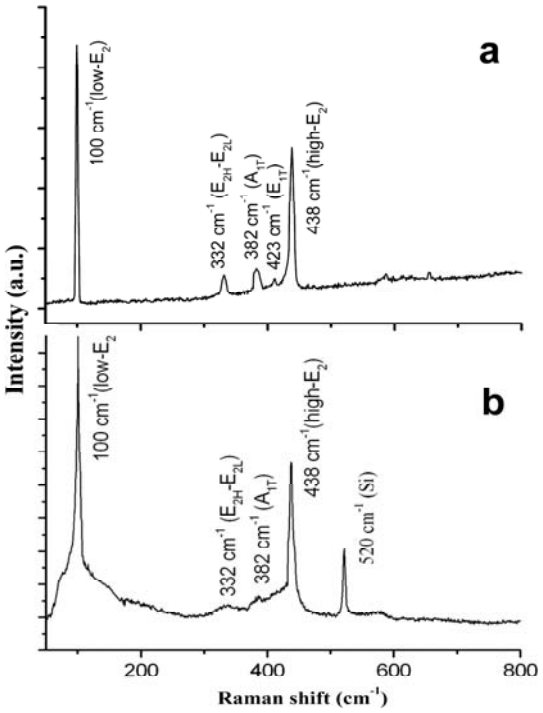

Figure 3: Micro-Raman scattering spectrum of (a) ZnO nanorods on glass substrate and (b) quasi-aligned ZnO nanorods on Si wafers grown under electric field assisted-assembly.

The multiphonon processes occur when phonon wave vectors are shifted away from the center of the Brillouin zone [15]. Another dominant peak at 100 cm^{-1} is commonly observed in the wurtzite structure ZnO [16] and is attributed to E_2(low) mode of non-polar optical phonons.

The weak peak is observed at 580 cm^{-1} of E_1(low) mode which show that our nanorod arrays have low quantity of impurities and structural defects (oxygen vacancies and Zn interstitials [17]).

4 CONCLUSIONS

This is a new report on electric-field assisted assembly technique used to vertically-align ZnO nanowires on the Si substrate during their growth in only 20 min. Well aligned ZnO nanorods were synthesized without employing any seeds, metal catalysts on glass and Si(111) substrates without any pre-coated buffer layers. The alignments of the ZnO nanorods on the different substrates depend on the growth conditions, substrate type and the strength of the applied electric-field. Similarly, the XRD, SEM and micro-Raman measurements showed the distinct appearance of ZnO nanorods on two types of substrates. Consequently, the crystal structure of ZnO nanorods is related to the type of the substrate and direction of electric field used.

To summarize, a technique for localized growth and alignment of ZnO nanorods on Si substrates to yield a assisted-assembled system has been demonstrated. This technique allows to ZnO nanorods synthesis and alignment using a DC electric-field. Enhanced control over ZnO nanorod alignment and organization is evident at higher field strengths. This process with its improved control yields a simple and reproducible fabrication method, which could be used in fabrication of nanodevices.

Acknowledgments The research described in this publication was made possible in part by Award No. MTFP-1014B Follow-on of the Moldovan Research and Development Association (MRDA) and the U.S. Civilian Research and Development Foundation (CRDF). Dr. L. Chow acknowledges partial financial support from Apollo Technologies Inc and Florida High Tech Corridor Program.

REFERENCES

[1] S. Choopun, H. Tabata, T. Kawai, J. Cryst. Growth 274, 167, 2005.
[2] O. Lupan, G. Chai, L. Chow, Microelectron. J. 38, 1211, 2007.
[3] M. Huang, S. Mao, H. Feick, H. Yan, Y. Wu, H. Kind, E. Weber, R. Russo, P. Yang, Science 292, 1897, 2001.
[4] X. F. Duan, Y. Huang, Y. Cui, J. F. Wang, C. M. Lieber, Nature 409, 66, 2001.
[5] R. Hauschild, H. Kalt, Appl. Phys. Lett. 89, 123107, 2006.
[6] M. Yan, H. T. Zhang, E. J. Widjaja, R. P. H. Chang, J. Appl. Phys. 94, 5240, 2003.
[7] J. Henzie, J. Barton, C. Stender, T. Odom, Accounts of Chemical Research 39, #4, 2006, p.249
[8] J. W. P. Hsu, Z. R. Tian, N. C. Simmons, C. M. Matzke, J. A. Voigt, J. Liu, Nano Letters 5, 83, 2005.
[9] O. Lupan, L. Chow, G.Chai, B. Roldan, A.Naitabdi, H. Heinrich, A. Schulte, Mater. Sci. Eng. B 145, 57, 2007.
[10] Joint Committee on Powder Diffraction Standards, Powder Diffraction File No 36-1451.
[11] A. Nahhas, H. K. Kim, J. Blachere, Appl. Phys. Lett. 78, 1511, 2001.
[12] J. S. Suh, K. S. Jeong, J. S. Lee, I. Han, Appl. Phys. Lett. 80 2392, 2002.
[13] (a) K. A. Alim, V. A. Fonoberov, M. Shamsa, A. A. Balandin, J. Appl. Phys. 97, 124313, 2005.
(b) M. Rajalakshmi, A. K. Arora, B. S. Bendre, S. Mahamuni, J. Appl. Phys. 87, 2445, 2000.
[14] C. Bundesmann, N. Ashkenov, M. Schubert, D. Spemann, T. Butz, E. M. Kaidashev, M. Lorenz, M. Grundmann, Appl. Phys. Lett. 83, 1974, 2003.
[15] T. C. Damen, Phys. Rev. 142, 570, 1966.
[16] Y. J. Xing, Z. H. Xi, Z. Q. Xue, X. D. Zhang, J. H. Song, R. M. Wang, J. Xu, Y. Song, S. L. Zhang, D. P. Yu, Appl. Phys. Lett. 83, 1689, 2003.
[17] K. Vanheusden, W. Warren, C. Seager, D. Tallant, J. Voigt, B. Gnade, J. Appl. Phys. 79, 7583, 1996.